Heat Extraction and Droplet Impact Regimes Obtained with Continuous Casting Air-mist Nozzles

Tania M. Flores F.[1], A. Humberto Castillejos E.[1], Brian G. Thomas[2]

[1]Laboratory of Process Metallurgy
Centro de Investigación y de Estudios Avanzados, CINVESTAV - Unidad Saltillo
Av. Industria Metalúrgica 1062, Parque Ind. Saltillo-Ramos Arizpe
Ramos Arizpe, 25900, Coahuila, Mexico
Phone: (+52 844) 438 9600, exts. 8666, 8685
Email: tania.flores@cinvestav.edu.mx
Email: humberto.castillejos@cinvestav.edu.mx

[2]Department of Mechanical Engineering
Colorado School of Mines
Brown Hall W370-B
1610 Illinois Street, Golden, CO 80401
Phone: 303-273-3309
Email: bgthomas@mines.edu

Keywords: Air-mist cooling, Steady state heat flux measurement, Visualization of drops in mists, Drop impact regimes

ABSTRACT

This work presents experimental results about heat extraction and drop impact regimes taking place when a local portion of a horizontal flat-fan air-mist jet impinges a metallic disk maintained at temperatures of interest to continuous casting. The mists were generated with a nozzle operating under conditions of practical interest, and the disk was placed at center and off-center positions located along the major axis of the mist footprint. These conditions cover a wide spectrum of mist characteristics. The heat flux correlated very well with average properties of free non-impinging mists. Visualization of mist-wall interaction using a high speed camera, aided by laser illumination, reveals different droplet impact regimes that influence intensity, efficiency and uniformity of the cooling process.

INTRODUCTION

In continuous casting, the steel strand is subject to several cracking problems during its passage through the secondary spray cooling system, e.g., transverse midface and corner cracks, or to exacerbation of longitudinal cracks that originated in the mold.[1] Often, these quality problems arise from spraying conditions that are unable to meet the cooling requirements demanded by changes in casting speed, mold powder behavior, or slab width. With the widespread use of hydraulic nozzles, even with pneumatic nozzles most operations simply scale the water flow rate with casting speed. With independent adjustment of air and water flow rate, pneumatic nozzles offer a wider range of possibilities for adjusting the cooling to variations in process conditions and should be harnessed to fully exploit their possibilities.[2] Effective adjustment of pneumatic nozzles requires knowledge about how mist properties - droplet size, droplet velocity and water impact density distributions – vary with operating conditions, and influence heat extraction. This requires understanding of the modes in which droplets in the mist interact with the surface to remove heat, which operate via different mechanisms.

Previous studies on air-water mist cooling have focused mainly on heat transfer measurement[3-7] and only few attempts have been directed towards investigating the interactions that take place when mists of interest to continuous casting of steel impinge against a solid surface.[8,9] Heat flux measurements have involved both steady-[3,5] and unsteady-state[6,7] methods. In steady experiments, a specimen is heated by a thermal power source to balance the heat extracted by the spray and maintain a constant temperature during the test. Thus, knowing the power input or a temperature gradient allows determination of the boiling convection heat flux, $-q$, and the surface temperature, T_w. In unsteady-state experiments, temperature-time histories

are measured near the surface for solving the inverse heat conduction problem to estimate $-q$ and T_w. Previous work using an electromagnetic induction-heated probe developed by the authors has been used to determine steady-state heat flux under spray and mist conditions of interest to steel continuous casting.[10,11] This method has the inherent advantage of decoupling surface temperature and time, which can be controlled and adjusted independently during a test.

The hydrodynamics of the impact of droplets in continuous-casting mists have been studied using direct visualization.[8,9] Under room temperature conditions a particle droplet image analyzer was used to determine the size and velocity of primary (arriving) and secondary (departing) drops moving in the vicinity of a solid surface; in addition, the thickness of the liquid film that builds up on the surface by accumulation of water was measured.[8] A recent work reported the interaction of drops in mists with a solid surface at high temperatures and suggested that the interaction of the drops with the surface depends on the impinging Weber number, $We_z\ (=\rho u_z^2\ d_d\ /\sigma)$.[9] Most of these observations have focused on single droplets[12] or droplet streams,[13] where properties of inflight drops, as well as hydrodynamic and thermal conditions of the surface, differ markedly from the spraying conditions encountered in continuous casting of steel.

In this work, the steady-state probe developed by the authors is used to investigate both droplet-surface interaction phenomena and heat extraction, during spraying conditions relevant to continuous casting, where film boiling prevails.

EXPERIMENTAL METHODOLOGY

To measure the local heat flux extracted by specific zones of a mist impinging over a hot surface, an electromagnetically induction heated probe is used in this work. The probe is schematically shown in Fig. 1(a) and is made of a Pt-disk (~ 8 mm × 2.7 mm thickness); an R-type thermocouple (0.5 mm) welded to the center of the disk back surface; an induction coil; and a ceramic body cast over the other components to isolate them thermally and leave just the disk front face exposed to the mist. To prevent moistening the ceramic is waterproof painted and, as seen in the figure, the probe assembly is encased in a Plexiglas tube which has a quartz window with a central hole in its front to expose the surface of the metal disk (probe). The disk protrudes 0.3 mm from the window to enable side views of mist events occurring on the disk surface and its vicinity. The location of the probe in relation to the center of the nozzle orifice is illustrated in Fig. 1(b), which shows that the setback distance is held constant, and the position along the major axis of the mist footprint is varied, setting x equal to 0 and 0.125 m, to highlight the influence of the droplet impingement angle on heat transfer and droplet-surface interactions. The schematic of the whole experimental rig presented in Fig. 1(c) shows that the coil, in the probe assembly, is connected to a high frequency generator (Luzars DX5-A, ASEPSA S.A. de C.V., QRO, Mexico), with 5 kW capacity. The generator is interfaced to a digital controller for adjusting the output power and maintain steady the specified setup temperature, T_m, at the back of the disk, under the different spraying conditions investigated. The root mean square current, RMSC, circulating through the coil is measured with a high frequency ammeter. The values of RMSC and T_m are used to calculate T_w and the overall heat flux extracted from the surface; the boiling convection heat flux, $-q$, is obtained by subtracting radiation losses from the overall heat flux. Details of the procedure used for estimating $-q$ and T_w are presented elsewhere.[14] The temperatures T_m maintained in the sample vary from 500 to 1200 °C to cover the film boiling regime.

As part of the study, the distributions of diameters, d_d, and normal velocities, u_z, of droplets in free mists are determined in sampling volumes A and B, indicated in Fig. 1(b), using a particle droplet image analyzer (Oxford Lasers, VisiSizer N60V, Oxford Lasers Ltd., Didcot, United Kingdom). The number of droplets, N, in the samples exceeds 5500 to ensure obtaining statistically meaningful average quantities. The quantities selected to represent the size and velocity of droplets are the volume mean diameter, d_{30}, and the volume weighted mean velocity, $u_{z,v}$, defined, respectively, as,

$$d_{30} = \left(\sum_{i=1}^{N} d_{d,i}^3 / N\right)^{1/3} \tag{1}$$

and

$$u_{z,v} = \left(\sum_{i=1}^{N} u_{z,i} d_{d,i}^3\right) / \sum_{i=1}^{N} d_{d,i}^3 \tag{2}$$

The other quantity measured in free mists is the water impact density, w, defined as the volume of water, v_d, passing through the projected area $a \times \cos(1 - \square)$ during a representative period of time t, as given by the following expression,

$$w = \frac{v_d}{t \cdot a \cos(1-\alpha)} \tag{3}$$

this quantity was measured using collecting tubes in a patternator.

Once steady state conditions are establish at each temperature, high-speed images of the interactions of drops with the surface are recorded. This is achieved using a high speed camera (FASTCAM SA3, Photron Ltd., Tokyo, Japan) interfaced to a pulsed diode laser (FireFLY FF50000, Oxford Lasers Ltd., Didcot. U.K.) equipped with a high-intensity diffuser. The orientation of the camera and laser is illustrated in Figure 1(c). A recording rate of 10000 fps is used with a shutter speed of 1/500000 seconds, obtaining an image resolution of 512×128 pixels, with a pixel size of 12 m. To minimize the through-thickness path to the focal plane and thereby enhance visibility, the fan of mist emerging from the nozzle was oriented vertically as illustrated in Figure 1(b). Additionally, as shown in the Fig. 1(c), a screen was used to narrow down the mist fan thickness so that just a slice of the fan reaches the heat measuring probe; it was verified that the screen does not modify *w* at the probe site. The captured images are very complex, so computer-automated image recognition of the droplets could not be used. Thus, the video recordings are analyzed by the naked eye running the films at low speed. The equivalent diameter and velocity of selected droplets are then determined using the software package Tracker.[15]

Table 1 lists the nozzle operating conditions and probe positions used in the experiments together with the corresponding average values of mist characteristics, i.e., d_{30}, $u_{z,v}$ and *w*. The air-mist nozzle used in the experiments is a Delavan W19822.

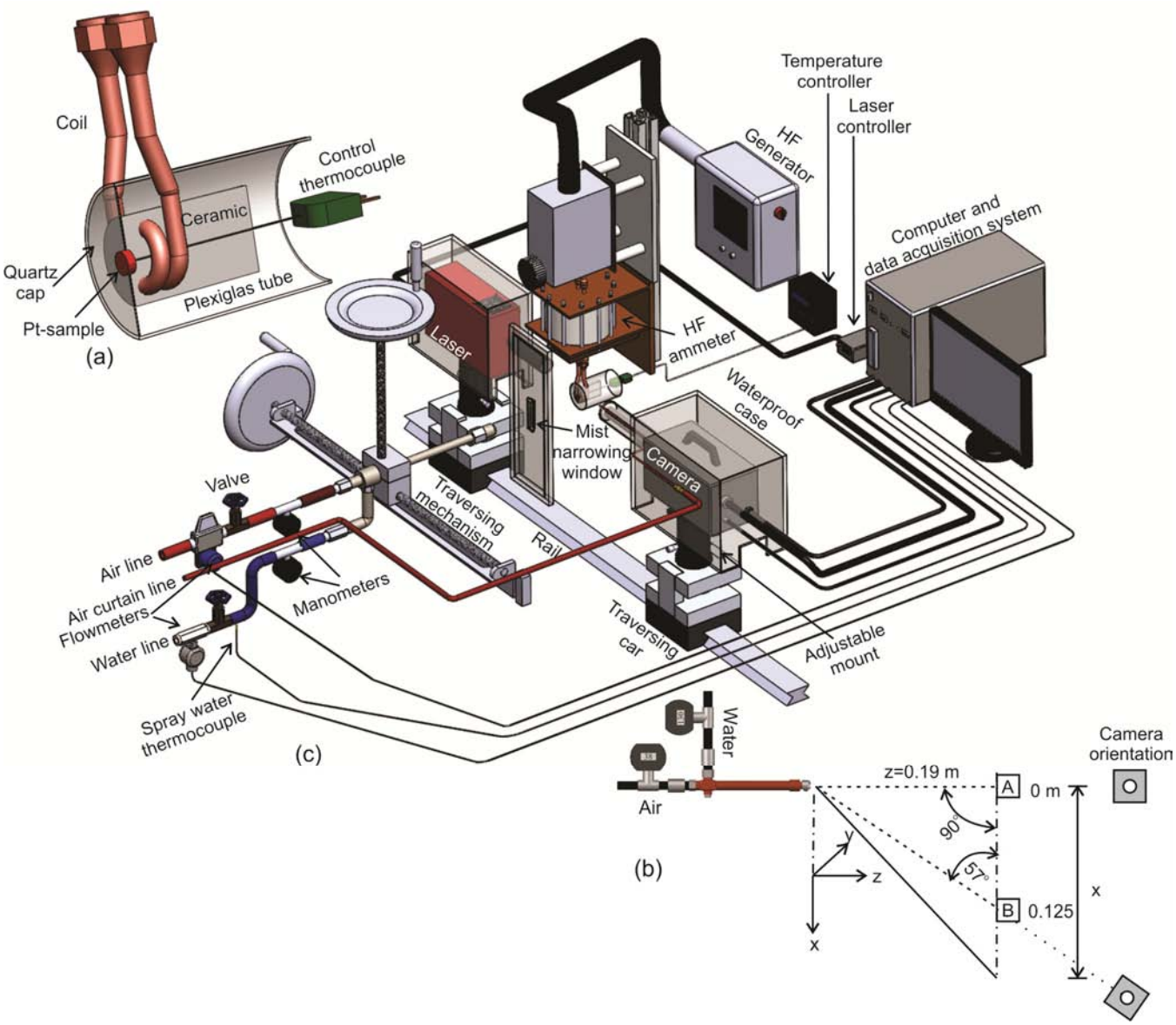

Fig. 1. (a) Heat flux measuring probe; (b) schematic of probe positions, showing nominal droplet impingement angles and camera orientation; (c) schematic of experimental set-up for measuring steady-state heat flux and visualizing droplet impingement phenomena.

RESULTS AND DISCUSSION

Experimental and Predicted Film Boiling Curves

The curves in Figs. 2(a) and 2(b) present the film boiling region, i.e., the upper temperature region, of boiling curves up to 1200 °C;[14] the minimum in the curves corresponds to the Leidenfrost temperature, T_L, and the symbols represent the average heat flux of at least two nonconsecutive experimental runs.

Table 1 - Experimental conditions: nozzle operating conditions, *x*-positions and local averaged hydrodynamic characteristics of droplets passing through the virtual impingement plane.

A, NL/s	p_a, kPa	W, L/s	x, m	$u_{z,v}$, m/s	w, L/m^{2}s	d_{30}, m
0.26	189	0.076	0	22.3	21.1	51.3
1.65	480		0	35.2	20.6	32.1
0.26	189		0.125	14.3	7.1	56.6
1.65	480		0.125	19.1	17.6	32.1

Figures 2(a) and 2(b) compare the effect of air-nozzle pressure, p_a, at a single water flow rate, W, on the heat flux removed by the mist at the center of the mist footprint, x= 0.0 m, and at an external position, x= 0.125 m from the fan centerplane, respectively. These graphs show that the air nozzle pressure has a very important influence on the heat extracted by the mist. Notice in Table 1 that increasing air pressure is accompanied by an important increase in $u_{z,v}$ and decrease in d_{30}, for this water flow rate, and also causes a substantial increase in w at external positions. This spatial variation in mist characteristics hints at extensive changes in the heat flux extracted from the entire fan footprint, at least for these nozzle conditions. Also, the nozzle operating conditions change how the heat flux varies with temperature.

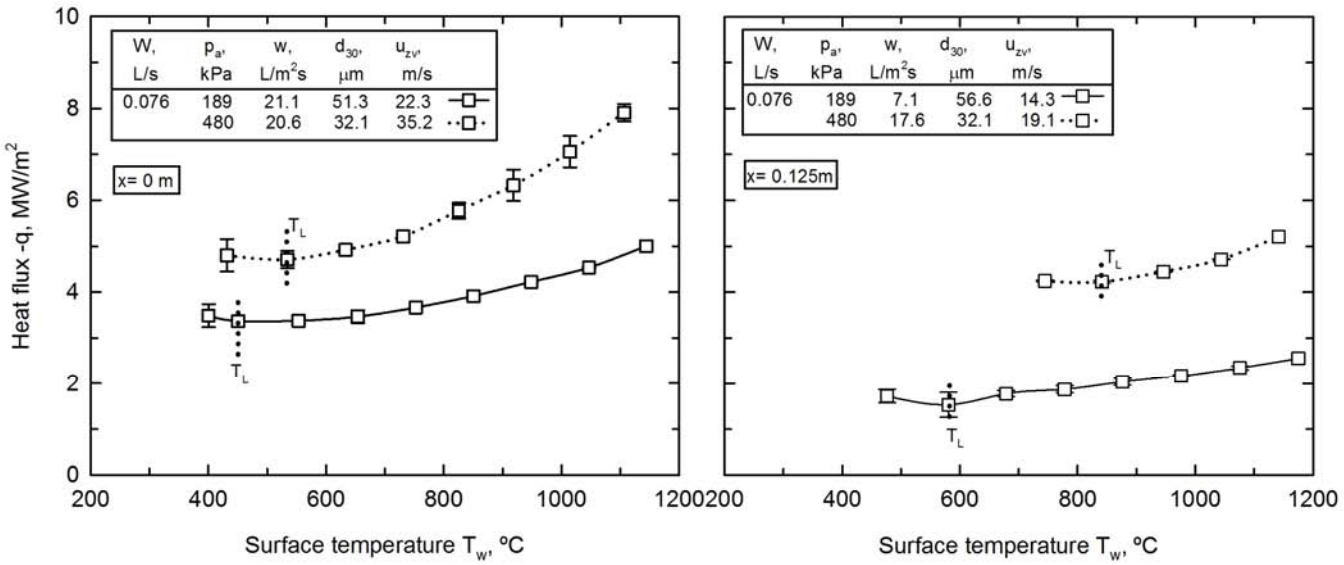

(a) (b)

Fig. 2. Mist heat flux curves corresponding to the film boiling regime for nozzle conditions specified and two *x*-positions: (a) 0.0 m; and (b) 0.125 m. The corresponding local values of w, d_{30} and u_{zv} are given in the legends.

Recently the authors[9] found that heat flux in the film boiling regime can be represented by the following power-law equation,

$$-q = 3\times10^{-3}\, w^{0.47}\, u_{z,v}^{0.42}\, T_w^{0.87}\, d_{30}^{-0.35} \tag{4}$$

This equation shows that heat flux in the film boiling regime increases with increasing water impact density, increasing volume-weighted mean velocity of droplets, increasing surface temperature and decreasing droplet volume-mean diameter. The accuracy of this fitting expression for predicting the boiling curves is shown in Fig. 3, for two widely different nozzle operating conditions and footprint positions. The discrepancy between measurements and predicted values is smaller than 20 %, and over large temperature ranges, the agreement is even better.

Droplet-Surface Interactions during Mist Impingement upon a Surface at High Temperature

As indicated previously, the nature of droplet interactions occurring on the surface of the Pt-disk and the motions taking place in its vicinity were investigated with the camera set-up given in Figure 1(c). This section shows a representative sample of fluid dynamic events observed under the nozzle operating conditions investigated, at positions x equals 0 and 0.125 m. At these two positions, the nominal impinging angle, α, varies from 90 to 57°, which significantly changes the normal impinging velocity, u_z and the droplet number flux,(droplets/m^{2}s). It also increases the droplet size, d_d.

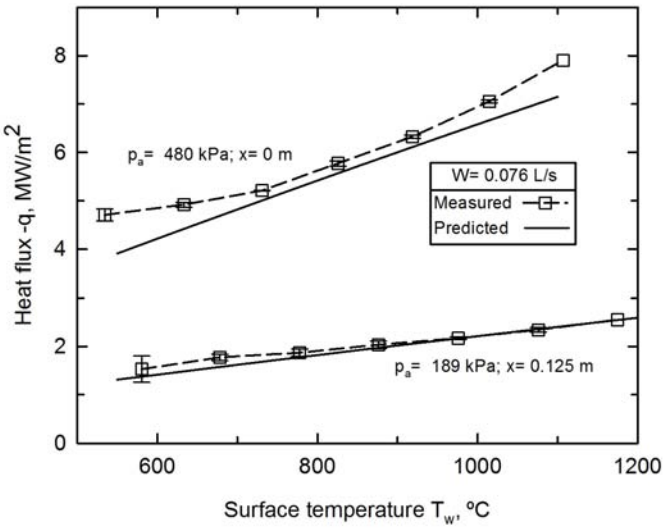

Fig. 3. Measured and regression estimated film boiling curves for the positions and conditions indicated.

Identifying the interaction modes of droplets in the mists is complicated because events occur very rapidly and the number density of droplets (droplets/m^3) is usually high. Both of these situations hinder observation.

Careful examination of the recorded videos at low speed reveals that droplets in mists travel as waves of parcels with low and high droplet concentration.[8] When visualizing low concentration parcels, four droplet-surface interactions modes are identified: (a) stick – the droplet deposits onto the wall in nearly spherical fashion; (b) spread – the droplet adheres to the surface, spreading and retracting until all of its energy is dissipated and it forms a film; (c) rebound – the droplet bounces off the surface after impact; and (d) splashing - the droplet initially impacts but while spreading becomes unstable, it spatters into fine secondary droplets. These different impinging modes observed in sprays are much like those reported in studies with individual droplets, but the rate at which they develop is much faster, and they occur consecutively (very rapidly one after another) or simultaneously, causing interference between droplets. Two splashing modes identified as fine and jet atomization were recognized and their characteristics are described below.

Figure 4 shows interaction modes that were mostly observed at the lateral position, x= 0.125 m, because they appear when droplets with low We_z impinges a hot surface; the surface in the figure appears inclined because the camera was tilted according to the nominal impinging angle of the droplets approaching the surface, as indicated in Figure 1(b). When low concentration parcels reach a surface at high temperatures there is a large probability that the surface is dry, because droplets move fast and also evaporate quickly. The stick mode is illustrated in Fig. 4(a) where it is clearly seen that in this regime, droplets settle gently on the surface maintaining approximately their size during the time they last in contact. In this regime droplets are seen to slide smoothly on the surface and levitate intermittently by formation of a vapor film underneath. This regime is observed to occur with droplets having $We_z < 4$.

The rebound mode appears also at low We_z, and is likely aided by the presence of vapor plumes originating from the interaction of previous droplets with the surface, and by the rapid formation of a vapor cushion underneath the impinging droplet, which pushes it away. Figure 4(b) shows a bouncing droplet that acquires a bowling pin shape when taking off from the surface. In general, droplets were observed to rebound when their $4 \leq We_z \leq 70$.

The spread mode appears rarely in the film boiling regime, but the large droplet number flux flowing through the sampling volume offers the possibility of finding this type of interaction, as seen in Figure 4(c). This sequence shows how a large non-spherical droplet approaches the surface slowly, touches, spreads, and retracts until a vapor film forms underneath it. These images indicate that even in the film boiling regime, vaporization of large droplets at low impinging We_z does not occur fast enough to forbid intimate contact of the liquid with the surface during a short period of time. Droplets in this regime have $70 \leq We_z < 100$ and their frequency of appearance is lower than the stick and rebound regimes.

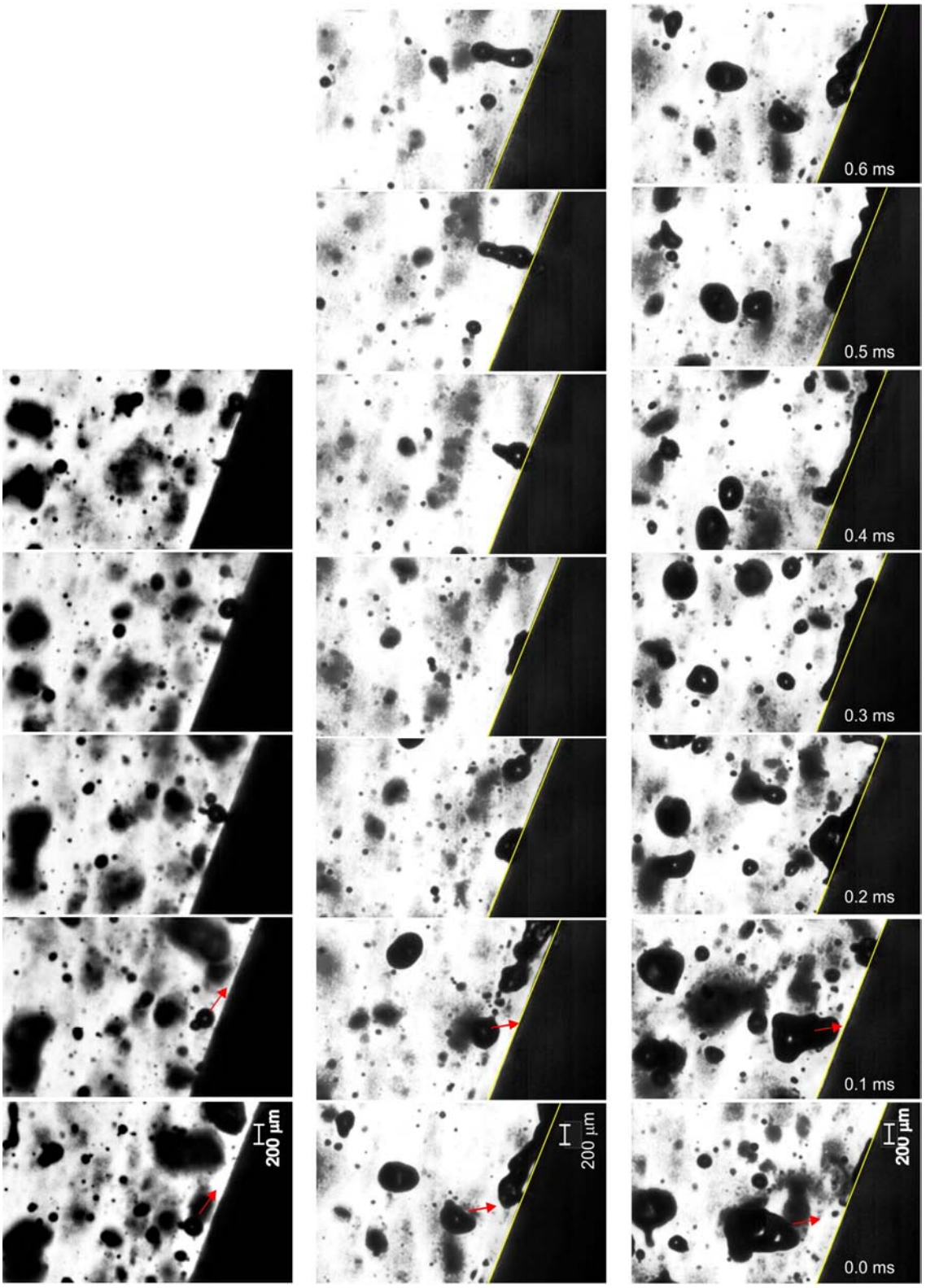

(a) (b) (c)

Fig. 4. Side view images of different drop impact modes indicating the particular droplet - d_d, u_z, We_z - and surface - T_w, -q - conditions involved: (a) stick – 160 m, 1.1 m/s, 2.5, 876 °C, 2.0 MW/m^2; (b) rebound – 254 m, 2.4 m/s, 20.4, 876 °C, 2.04 MW/m^2; and (c) spread – 518 m, 3.7 m/s, 96.2, 876 °C, 2.0 MW/m^2.

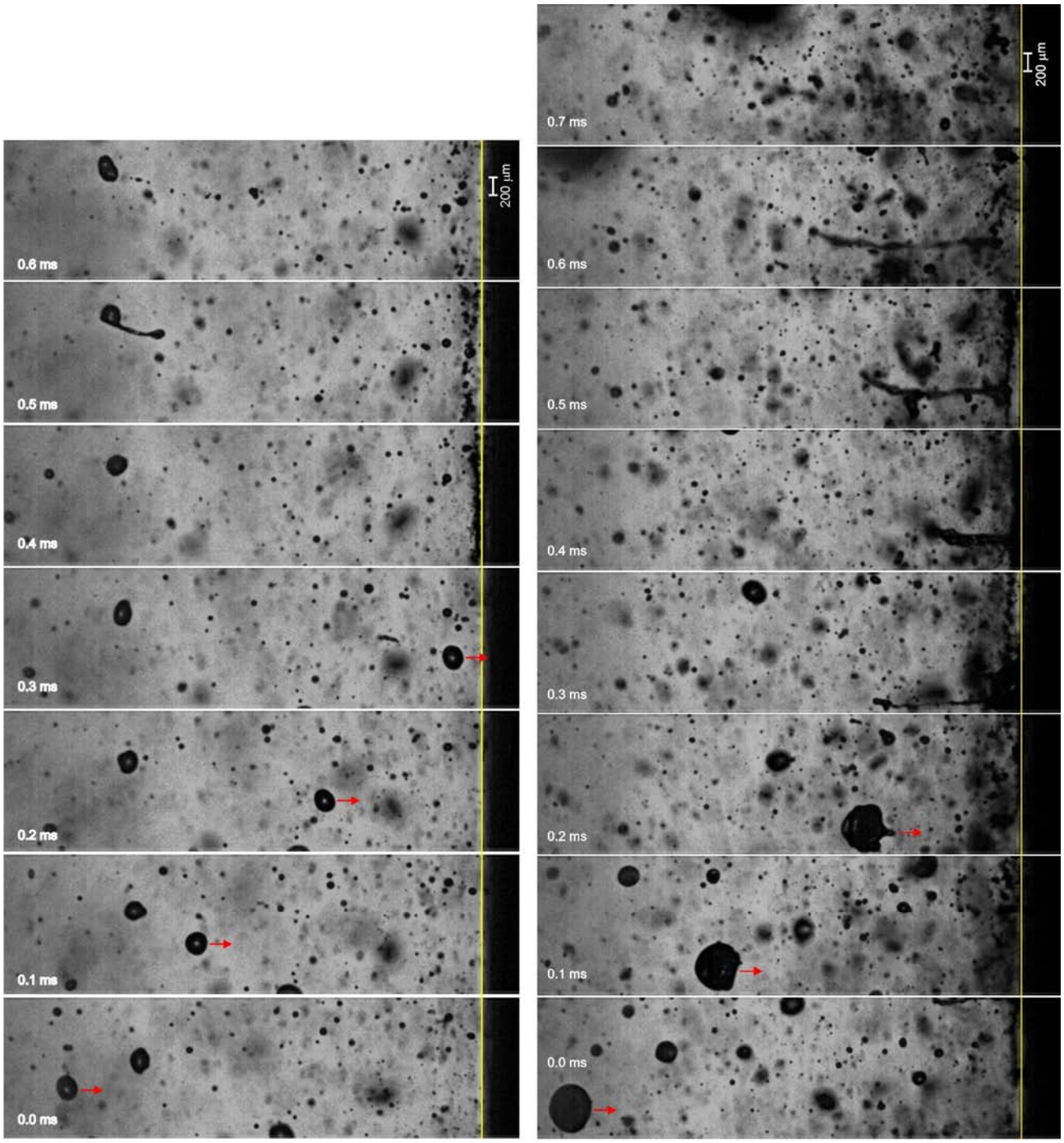

(a) (b)

Fig. 5. Side view images of different droplet impact modes indicating the particular droplet - d_d, u_z, We_z - and surface - T_w, -q - conditions involved: (a) splash with fine atomization, 374 m, 21.7 m/s, 2414, 1144 °C, 5.0 MW/m^2; and (b) splash with jet atomization, 762 m, 26.0 m/s, 7049, 850 °C, 3.9 MW/m^2.

The regimes of stick, rebound and spread also appear in the central footprint position but their probability of appearance is smaller, because the normal velocity of the droplets is larger so the chance of droplets with low We_z is smaller than at external positions.

Two splashing modes appear when droplets with high Weber number impact a surface at temperatures in the film boiling regime; they are splash with fine atomization and splash with jet atomization. Droplets exhibiting fine atomization upon impact are small highly energetic droplets that spread forming a thin lamella that is broken into many fine droplets by blows of formed vapor that emerge through it, as suggested by the sequence of images shown in Figure 5(a). From the figure is seen

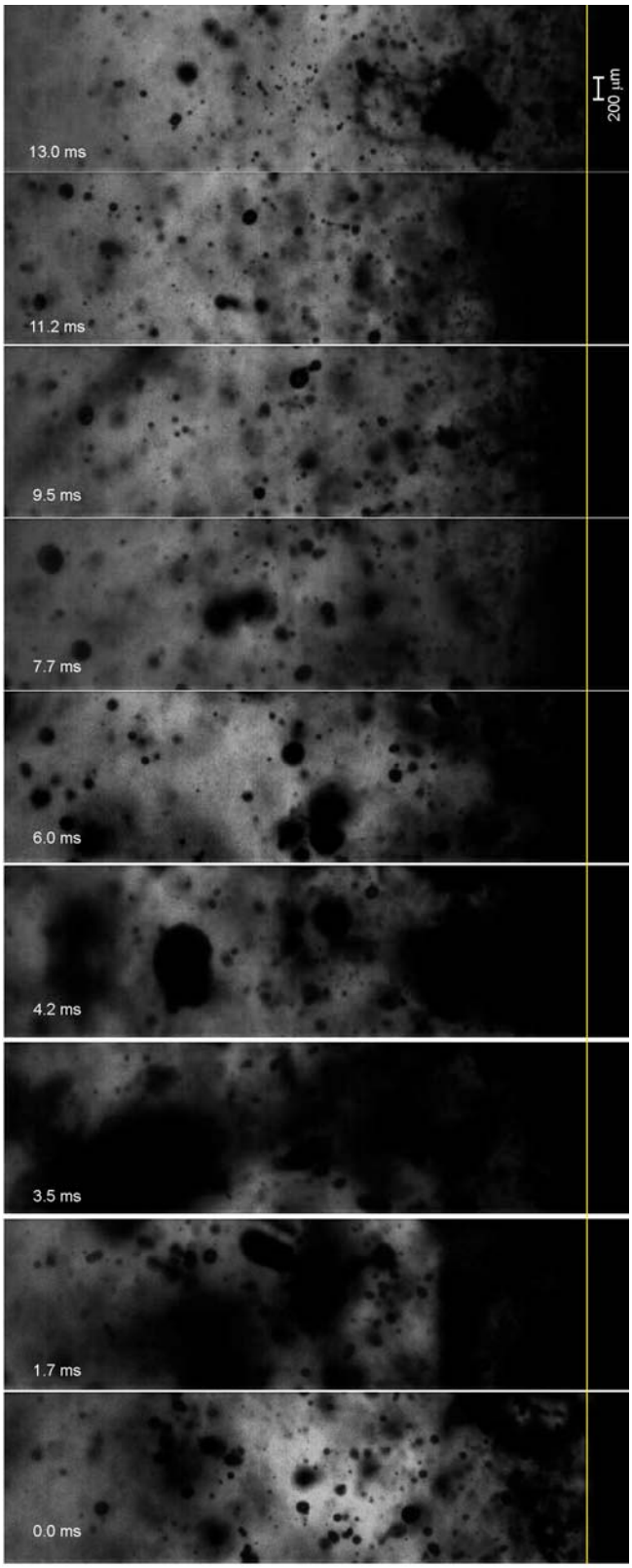

Fig. 6. Impact of dense parcels at x= 0 m, W= 0.076 L/s, p_a= 189 kPa, T_w= 1144 °C, -q= 5 MW/m^2.

that soon after impact the droplet has spread covering a length much larger than its diameter, suggesting that a thin film with a large area must establish intimate contact with the hot surface for a very brief period of time. During the brief period, lasting < 0.1 ms, vapor forms and breaks through the film producing fine secondary droplets that are separated, while moving parallel to the wall, very small displacement takes place in the perpendicular direction. The vapor film that levitates droplets

is the characteristic structure defining film boiling and in no way is a steady structure but forms intermittently in random sites. This regime is observed with small droplets, $d_d < 500$ m, having $We_z \geq 70$.

Big drops, $d_d \geq 500$ m that approach the hot surface with large normal velocity give rise to splash with jet atomization, such as shown in Figure 5(b). As seen in the figure, these large drops acquire a spherical cap shape as they approach the surface. The increase in pressure resulting from stagnation of the airstream and evolution of vapor deforms the front hemisphere of these large speedy drops as they approach the surface. Upon contact, the top of the impacting drop surges rapidly as tubules or veins, while lateral spreading on the surface does not occur. When large fast drops with no major lateral deformation suddenly stop upon contact with the surface, they likely cause a shock wave that produces the uprising jet observed in Figure 5(a). As time progresses, the jet continues to rise until it breaks into small secondary droplets. After the jet has formed the droplet spreads laterally to form a water layer that is levitated and broken into several secondary droplets, similar to the phenomena observed during splash with fine atomization. This regime is observed with large drops having $We_z \geq 1000$.

The five modes of interaction – stick, rebound, spread, splash with fine atomization and splash with jet atomization – appear over the entire mist impact area and it is the frequency with which they take place that marks the difference in heat flux over the mist footprint which, according to Figs. 2(a) and 2(b), can be quite important. The impact regimes identified with single droplets occur during short time periods where dilute parcels interact with surface. Dense parcels are more ubiquitous and during the time they last, droplets are able to build up thick liquid films on the surface. These films renew frequently and are vigorously agitated by impinging droplets. Figure 6 shows images of dense parcels over a period of time lasting 13 ms. This time lapse is much longer than the time occupied by dilute parcels, so the arrival of dense parcels is likely crucial in determining the rate of heat extraction. In some of the images shown in Fig. 6, it is possible to observe clear vapor regions over the surface (e.g., at 0 and 13 ms), although the liquid layer is usually thick and no vapor can be observed on the liquid-solid interface. However, vapor slugs appear to rise inside the liquid film (e.g., in the images at 1.7, 3.5, 6 and 11.2 ms).

CONCLUSIONS

This work presents experimental results on heat extraction and droplet impact regimes taking place when a local portion of a horizontal flat-fan air-mist jet impinges a metallic disk maintained at temperatures of interest to continuous casting. The mists were generated with a nozzle operating under conditions of practical interest, and the disk was placed at center and off-center positions located along the major axis of the mist footprint. It was found that the heat flux extracted, $-q$, is very well correlated in terms of $u_{z,v}$, w and d_{30} of free non-impinging mists in addition to T_w. Visualization of mist-wall interactions reveal that droplets in mist move as waves of low and high density parcels. In the first droplets interact with the surface as individual drops that may experience interference with droplets arriving previously or simultaneously, and give rise to five interaction modes: stick, rebound, spread, splash with fine atomization and splash with jet atomization. The interaction regimes are defined mainly by the value of We_z. On the other hand dense parcels flood the surface forming discontinuous films that renew rapidly and are well mixed by frequent impact of primary droplets and returning secondary droplets. Impingement of dense parcels play a crucial role in mist heat extraction.

ACKNOWLEDGEMENTS

We are grateful to the National Council of Science and Technology of Mexico (CONACYT) and the National Science Foundation (US) for financial support through grants No. 241103 and CMMI-1300907, respectively, and also to the Continuous Casting Consortium at the University of Illinois. TMFF express her gratitude to CONACYT for the award received for her Ph.D. studies.

REFERENCES

1. B.G. Thomas, J. Bentsman, B. Petrus, S. Vapalahti, H. Li, A.H. Castillejos, GOALI: Online Dynamic Control of Cooling in Continuous Casting of Thin Steel Slabs, Proc. *2008 NSF Engineering Research and Innovation Conference*, Knoxville, Tennessee.
2. J.J. Montes R., A.H. Castillejos E., E.P. Gutiérrez M. and M.A. Herrera G., Effect of the Operating Conditions of Air-Mist Nozzles on the Thermal Evolution of Continuously Cast Thin Slabs, *Canadian Metallurgical Quarterly*, 47, (2), (2008), 187-204.
3. I. Mudawar, W.S. Valentine, Determination of the Local Quench Curve for Spray-cooled Metallic Surfaces, J. Heat Treat., 2 (7) (1989) 107-121.
4. J. Schmidt, H. Boye, Influence of Velocity and Size of the Droplets on the Heat Transfer in Spray Cooling, Chemical Engineering Technology, 24 (3) (2001) 255-260.

5. C.A. Hernández B., A.H. Castillejos E., X. Zhou, B.G. Thomas, Measurement of Heat Flux in Dense Air-Mist Cooling: Part II. The Influence of Mist Characteristics on Steady-State Heat Transfer, Exp. Therm. Fluid Sci., (44) (2013), 161-173.
6. A.H. Castillejos E., M.A. Herrera, I. Hernández C., E.P. Gutiérrez M, Practical productivity gains – Towards a Better Understanding of Air-mist Cooling in Thin Slab Continuous Casting, in: Proceeding of the Third International Congress of Steelmaking, Association of Iron and Steel Technology, R. Guthrie, ed., Charlotte, N.C., (2005) 881–890.
7. H.M. Al-Ahmadi and S.C. Yao, Spray Cooling of High Temperature Metals using High Mass Flux Industrial Nozzles, Experimental Heat Transfer, 21 (1) (2008) 38-54.
8. M. De León B. and A.H. Castillejos E., Physical and mathematical modeling of thin steel slab continuous casting secondary cooling zone air-mist impingement, Metall. Mater. Trans. B, (46) (2015) 2028-2048.
9. M.E. Huerta L., M.E. Mejía G., A.H. Castillejos E., Heat Transfer and Observation of Droplet-Surface Interactions during Air-mist Cooling at CSP Secondary System Temperatures, Metall. Mat. Trans. B, (47) (2016) 1409-1426.
10. C.A. Hernández B., A.H. Castillejos E., X. Zhou, B.G. Thomas, Measurement of Heat Flux in Dense Air-Mist Cooling: Part I. A Novel Steady-State Technique, Exp. Therm. Fluid Sci., (44) (2013) 147-160.
11. Xiaoxu Zhou, Brian G Thomas, C. Alberto Hernandez; A. Humberto Castillejos E., Measuring Heat Transfer During Spray Cooling Using Controlled Induction-Heating Experiments and Computational Models, Applied Mathematical Modelling, 37, (2013), 3181-3192.
12. G.E. Cossali, M. Marengo, M. Santini, Secondary Atomisation Produced by Single Drop Vertical Impacts onto Heated Surfaces, Experimetal Thermal and Fluid Science, (29) (2005) 937-946.
13. G. Castanet, T. Liénart, F. Lemoine, Dynamics and Temperature of Droplets Impacting onto a Heated Wall, Int. J. Heat Mass Transfer, (52) (2009) 670-679.
14. Tania M. Flores F, Claudia Barraza de la P., A. Humberto Castillejos E., Steady-state Air-mist Heat Extraction and Visualization of Droplets-Surface Interactions from 60 to 1200 °C', (ISSN: 0894-1777), submitted to E*xperimental Thermal and Fluid Science,* February 2017.
15. Tracker Video Analysis and modeling tool, http://physlets.org/tracker/. Accessed 2015.